K 12/14

CONF-790800--36

EXPERIMENTAL SEISMIC TEST OF FLUID COUPLED CO-AXIAL CYLINDERS

MASTER

Mamerto L. Chu - Mechanical Engineering Dept.
The University of Akron

Sam J. Brown* Nuclear Equipment Division
The Babcock & Wilcox Company

Joseph F. Lestingi** - Mathematics and Mechanics Dept.
General Motors Institute

* presently with J. Ray McDermott & Co., Inc., R & D Division, New Orleans, La.
** formerly with the University of Akron, Civil Engineering Dept.

1. Introduction

The problem of the dynamic interaction between elastic deformation of a structure and the motion of a fluid in contact with the structure is encountered in numerous applications within the maritime, petro-chemical, aerospace and power generation industries. In this paper we will limit discussion to the dynamic response of fluid coupled coaxial cylindrical shells. There is particular interest in such problems within the nuclear industry with respect to the seismic design of the reactor vessel and thermal liner. Of course, similar structural configurations can be found in many other applications.

A review of the literature reveals many analytical contributions that assess the vibrational problem of fluid coupled coaxial cylinders. A list includes papers by Bowers, S. S. Chen, Horvay, Krajcinovic, Levin, Sharp-Wenzel, Au-Yang, Levy, Kalinowski, Everstine, Schroeder, Skop and many others. A few papers have treated the seismic problem analytically such as Citerly [1].

Experimental studies of vibrational characteristics of fluid coupled coaxial cylinders have been conducted by Levin and Milan [2], Au-Yang [3], Au-Yang and Skinner [4], and Mulchay et al [5]. With the exception of the Reference [5] test, the experiments were performed with relatively small radius-to-gap ratios [$\frac{\text{radius}}{\text{gap}} < 11$] ; and excluded seismic loading. Reference [5] considered one of the cylinders as rigid. Of the experimental

tests performed to study seismic solid-fluid interaction, they have been oriented to investigating sloshing effects in single cylinders such as reported by Kana, Dodge, and Clough. It was because of the limited experimental data available and the need to obtain experimental data for seismically loaded flexible fluid coupled coaxial cylinders with variable clearances (or gap) between the cylinders that the tests reported in this paper were undertaken. The purpose of the experimental data is to provide bench mark data to evaluate our analytical procedures. Large radius-to-gap ratios of about 55 were of interest because of prototype reactor-thermal liner design considerations.

The experiments described in this paper present a series of tests which investigate the effect of the annular clearance between the cylinders (gap) on natural frequency, damping, and seismic response of both the inner and outer cylinders. The seismic input is a time history base load to the flexible fluid filled coaxial cylinders. The outer cylinder is elastically supported at both ends while the inner cylinder is supported only at the base (lower) end.

2.0 Experimental Set-up

2.1 Test Cylinders - Four acrylic cylinders are used in this experiment. Table 1 gives both the material properties and nominal sizes of these cylinders. The 12-inch (308 mm) outer diameter acrylic cylinder used as the #3 inner cylinder is obtained as a cast cylinder while the remaining two inner cylinders (#6 and #9) with progressively lesser outside diameters are fabricated from acrylic sheets. The outer cylinder (#12) has an inner diameter of 13.625 inches (346.08 mm) and is rolled. The cylinders are of the same thickness (0.125 in.(3.175 mm)) and have maximum thickness and radius variation of 5% and 3.4% respectively. The cast cylinders show the least variation compared to the fabricated (rolled) cylinders. Figure 1 shows a photograph of the set up, illustrating the outer cylinder concentric with an inner cylinder. Figure 2 shows a schematic diagram of both outer and inner cylinders with appropriate dimensions. As illustrated both the acrylic caps (on inner cylinders) and flange (on outer cylinders) are 0.25 inches (6.35 mm) thick with six bolt holes in the caps and twelve bolt holes in the flange. The outer cylinder is bolted to the frame at each end, while the inner cylinder is left free at the top (inverted pendulum). Steel bolting annular rings are used for both outer and inner cylinders in order to circumferentially distribute the restraints. The flange and caps are designed so as to provide nearly rigid lateral restraints on the cylinder ends but allows relatively low rotational stiffness.

2.2 Frequency Test - Figure 3 shows the test frame for the determination of natural frequencies and damping ratios of the test cylinders. As shown, the test frame consists of three steel stands. One stand (central) is used to mount the cylinders while the stand on the left supports the 10 - lb. (44.5 N) shaker. The stand on the right prevents transverse relative motion of the cylinder ends. All frames are rigidly bolted on an isolated vibration test table, which minimized the influence of external excitations. The cylinders are 'point' excited through a horizontal rigid rod mounted on the shaker table.

2.3 Seismic Test - Figure 4 shows a photograph of the seismic test frame. As illustrated, the structure, which is fabricated from 3/8" (9.525 mm) thick tubular steel beams, is suspended from the laboratory ceiling with three flexible 1.5"(38.1 mm) hollow steel tubing. The 100 lbs. (445 N)CGS/Lawrence hydraulic shaker is mounted horizontally to a massive steel structure, with the actuator shaft hinged to the seismic test structure at mid-height for seismic input.

3.0 Instrumentation

3.1 Frequency Test - Figure 5 shows a schematic of the experimental setup for the frequency and damping tests. As shown, the outer cylinder is 'point' excited by the 10-lb (44.5 N) shaker which was controlled by a B & K vibration exciter. Constant force excitation is maintained by a feedback loop from a load cell mounted in series with the exciting rod. The frequency of oscillation of the cylinder is monitored by a B & K mini-accelerometer mounted on the surface of the cylinder. The mode shapes of the displacement responses are mapped by two roving eddy current probes. The outer cylinder is mapped on the outer surface and the inner cylinders on the inner surfaces. The annular gap is filled with tap water.

3.2 Seismic Test - Figure 6 provides a schematic of the instrumentation used in this test. The time history dynamic responses, of both inner and outer cylinders, due to a simulated seismic input are monitored by two types of instrumentation. For the acceleration response two mini-accelerometers are mounted approximately 4 inches (101.6 mm) from the top of the cylinders. For displacements relative to the frame, two eddy current probes are used (pointed at approximately the same locations as the acceleration test).

4.0 EXPERIMENTAL PROCEDURES

Table 2 lists the series of tests performed in this study. These tests are designed to determine the influence of the annular gap size on the resonant frequencies, damping ratios, mode shapes and the relative dynamic response of the inner and outer cylinders due to seismic-loading.

4.1 Frequency Test

The approximate resonant frequencies of each cylinder system i.e, an inner and outer cylinder combination, are first determined using the standard "sweeping" technique. The outer cylinder is excited from 5 Hz to 1k Hz at a slow sweeping rate ($\simeq$ 40 Hz/min.). The peaks of the r.m.s. spectral plot of the response from a stationary eddy probe opposite the excitation point (anti-node) inside the inner cylinder provide the approximate locations of the resonant frequencies of a cylinder system. The "exact" resonant frequencies are then pinpointed by vernier scanning in the vicinity of the "peaks". Three to four of the lowest resonant frequencies are determined for each cylinder system. A typical spectral plot is shown in Figure 7 for a sinusoidal excitation.

After the resonant frequencies are "pin-pointed", the phase relationship between the inner and outer cylinder responses at a particular frequency is determined by simultaneously displaying both signals on a dual trace scope. The mode shapes are then determined by mapping with an eddy probe pointed at the metal disks which are positioned circumferentially every 10^{o} at one quarter length locations as well as axially every 1.5 inches (38.1 mm) at 90^{o} circumferential locations. Figure 7 shows typical mode shapes.

The half-power point technique as given by Thompson (6) is used to determine the viscous damping ratio for a given natural mode. The damping ratio as developed for the half-power point technique is:

$$\varepsilon \simeq \frac{f_{b_1} - f_{b_2}}{2f_n}$$

where f_n = natural frequency with a response x_n

f_{b_1} = lower side band frequency with a response,

$$x_{b_1} = 0.707\ x_n$$

f_{b_2} = higher sideband frequency with a response,

$$x_{b_2} = 0.707\ x_n$$

The response x_n is first measured by an eddy probe at the antinode for a given natural frequency f_n. Then the sideband frequencies f_{b_1} and f_{b_2} are obtained by "Vernier" scanning of both the left and right sides of the "peak" where the responses are $0.707\ x_n$ as read through a digital meter. Variation of damping ratios with gap for the three cylinder combinations of test series 3 is shown in Figures 8 and 9.

4.2 Seismic Test

Figure 6 is a schematic of the instrumentation used in this study. A simulated seismic signal with low frequency content (2 - 30 Hz) is first formulated and used as input to the control unit of the CGS/Lawrence hydraulic shaker. Time histories of both acceleration and displacement responses from the inner and outer cylinders are recorded simultaneously in analog form using an F.M. tape recorder.

The recorded signals are then converted into digital form and used as input data for a digital program using an I.B.M. computer. Time history waveforms for both acceleration and displacement are plotted out by a Calcomp plotter. Spectral plots for the acceleration responses are also plotted using a fast Fourier transform. Absolute acceleration and relative displacement plots are shown in Figures 10 and 11, respectively. Cylinder accelerations are obtained from accelerometers which measure any change in acceleration of monitored points relative to a global absolute point. The cylinder displacements are computed relative to the base of the cylinders (support frame). Figure 12 shows the Spectral Plot. Both R.M.S. and peak acceleration ratios of inner cylinder to outer cylinders dynamic responses are also computed and are shown in Figure 10.

5.0 RESULTS AND OBSERVATION

Table 3 shows the natural frequencies of each of the four cylinders in air. As expected the frequencies for a given mode decrease as the diameter increases.

During the test series 2 and 3, the two distinct responses, in-phase and out-of-phase vibration from each cylinder, were observed.

In the in-phase motion both the inner and outer cylinders move radially in the same direction, for a given shell mode, while in the out-of-phase, the inner and the outer cylinders moved in the opposite radial direction. Figures 8 and 9 illustrate the variation of frequency (solid lines) with the annulus gap size, for the in-phase and out-of-phase responses.

The figures show that for the in-phase response, the frequency increases as the gap size decreases (Fig. 8) while for the out-of-phase mode the natural frequencies decreases as the gap size decreases. It is also seen that the resonant frequency is a non-linear function of the gap size. This phenomena could be attributed to the fluid viscous effects, i.e., during the out-of-phase mode as the gap size decreases, tangential flow of the fluid becomes more restricted, thus the tendency to eliminate the out-of-phase modes while for the in-phase mode, tangential flow is negligible hence as the gap decreases the two cylinders tend to act as one cylinder with the effective thickness increase resulting in a frequency increase.

Figures 8 and 9 also show the variation of damping ratios (ξ) with gap (dashed lines). The results indicate that for the in-phase modes the damping ratios generally remain within the 4-5% range as the gap size becomes smaller, but for the out-of-phase modes it increases significantly from 5% to 15% as the gap decreases. This is attributed to the fact that as the gap decreases, viscosity effect of the tangential fluid flow becomes more significant.

Figures 10 and 11 show respectively the acceleration and displacement responses of the three combinations of inner and outer cylinders, subjected to a simulated seismic loading. As can be seen in both figures, the amplitude response of the inner cylinder decreases as the gap decreases, while the

response of the outer cylinder remained relatively unaffected. The contrast between their responses is more obvious in the displacement response Fig. 11. The R.M.S. Ratio (referred as the R.M.S. response of inner to the R.M.S. response of the outer cylinder) are shown, vary from 16.8 for the widest gap (0.9375")(23.81 mm) to 2.78 for the smallest gap (0.125") (3.175 mm). In these tests, the inner cylinder was mounted as an inverted pendulum, (i.e. bolted to the frame at the bottom end only). Thus when the gap decreases, the viscosity effect of the fluid due to restricted passageway, damped out the motion of the inner cylinder, while the outer cylinder was relatively unaffected due to its large dynamic mass and relatively rigid connection with the frame (bolted at both ends). In Figure 11, the outer cylinder displacement scale is greatly magnified. Figure 12 shows a superposition of the spectrum responses for the three gaps considered. As shown, both the frame (dots) and the outer cylinder (solid lines) responses are almost identical. But the frequency response of the inner cylinder (dashed lines) varies as the gap changes. In general the inner cylinders have higher responses compared to the outer cylinder at low frequencies, and lower responses at higher frequencies. However the "cross over" frequency (i.e. from higher to lower) tends to decrease as the gap decreases, at around 18Hz for the widest gap down to about 13Hz for the smallest gap. At the smallest gap, the difference in response between

the inner and outer cylinder is at its lowest. This observation tends to convey the idea, that as the gap decreases, the pendulum or beam motion of the inner cylinder tends to be damped out. Referring to Figures 11 and 12, it is apparent that at the small gap the response is a higher frequency shell response, whereas the #12-#3 and #12-#6 cylinder combinations exhibit a predominant low frequency response of the inner cylinder that can only be the pendulum or beam mode.

The results of these experimental studies are intended primarily as benchmark test case data for qualification of analytical seismic analysis methods. Also, some insight into the actual response of fluid-coupled co-axial cylinders to seismic excitation can be developed from the test results. Analytical studies based on the geometries, materials and seismic loads used in these experiments are in progress and will be reported in future papers.

6.0 ACKNOWLEDGMENTS

The authors would like to thank the Clinch River Breeder Reactor Project for funding of the tests performed in the paper as well as the Babcock & Wilcox Company and the Westinghouse Advanced Reactor personnel associated with the project for their valuable comments. The data reported in this paper represents a portion of the 94 experimental tests and analytical finite element comparisons performed in the scope of the overall project.

7.0 References

[1.] "Response of a Cylindrical Fluid Container to Seismic Motion", by R. L. Citerly, et al., ASME, Pressure Vessel and Piping Div., 76-PVP-28, 1976.

[2.] "Coupled Breathing Vibrations of Two Thin Cylindrical Co-Axial Shells in Fluid," Vib. Problems in Industry, Intn'l Symposioum, Keswick, England, 1973.

[3.] "Response of Reactor Internals to Fluctuating Pressure Forces", M. K. Au-Yang, Nuclear Engineering and Design 35 (1975).

[4.] "Effect of Hydrodynamic Mass Coupling on the Response of a Nuclear Reactor to Ground Acceleration", M. K. Au-Yang and D. A. Skinner, 4th Int'l Conference on SMIRT, 1977.

[5.] "Analytical and Experimental Study of Two Concentric Cylinders Coupled by a Fluid Gap," T. M. Mulchay, et al., 3rd Intn'l Conf. on SMIRT, Sept. 1975, London, England.

[6.] "Vibration Theory and Application", W. T. Thomson, Prentice-Hall, Inc., Englewood Cliffs, N. J.

LIST OF TABLES

Table 1 TEST CYLINDERS

Cylinder	Material	OD(in)	ID(in)	t(in)	R/t	L(in)	Type*	Code**
3	acrylic	12.0		0.125	48	24	E	I_{13}
6	acrylic	13.0		0.125	52	24	R	I_{23}
9	acrylic	13.625		0.125	54.5	24	R	I_{33}
12	acrylic		13.875	0.125	56.5	24	R	O_3

* E = extruded (catalogue item)
R = rolled (special order)

** I = inner cylinder
O = outer cylinder

TABLE 2 TESTING PROGRAM

Test Series	Description	Purpose	Boundary Cond.	Tests
1	O_3, I_{i3} in air	Frequencies	O_3(SS), I_{i3}(P)	4
2	O_3 with I_{i3} (water in gap)	Frequencies & Damping Ratios	O_3(SS), I_{i3}(P)	3
3	O_3 with I_{i3} (water in gap)	Seismic	O_3(SS), I_{i3}(P)	3

(SS) = simple support

(P) = cantilever (pendulum)

i = 1, 2, 3 (refer to Table I for code)

TABLE 3

Cylinder	Frequency (Hz)			
I_{13}(P)	40.9 (1,1)†	77 (3,1)	148 (5,1)	198 (5,1)
I_{23}(P)	29.5 (1,1)	92 (3,1)	146 (3,1)	186 (4,1)
I_{33}(P)	21.3 (1,1)	109 (2,1)	119 (6,1)	142 (3,1)
O_3(SS)	128 (3,1)	167 (4,1)	215 (5,1)	327 (6,3

P - Pendulum support (cantilever)

SS - Simple support

All cylinders are 0.125" thick.

	(1,1)	(2,1)	(3,1)	(4,1)
I_{13}(P,SS)	40.9	*	148,132	198,183
I_{23}(P,SS)	29.5	*	146,129	186,174
I_{33}(P,SS)	21.3	*	142,128	170.159
O_3(SS)	--	*	128	167

† Numbers in parentheses indicate circumferential and longitudinal modes respectively.

* Analytical studies indicate that (2,1) frequencies are close to (4,1) which may account for their absence.

Figure 1 Acrylic and Inner Steel Cylinder

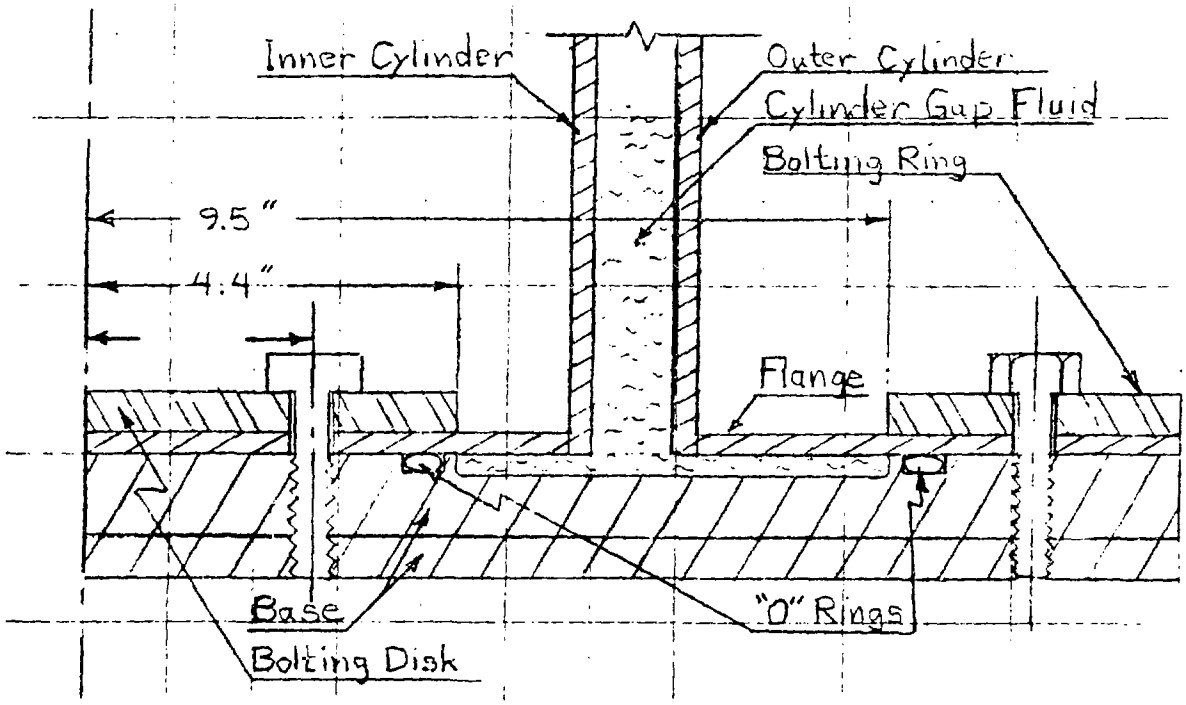

Figure 2 Cylinder Support Configuration

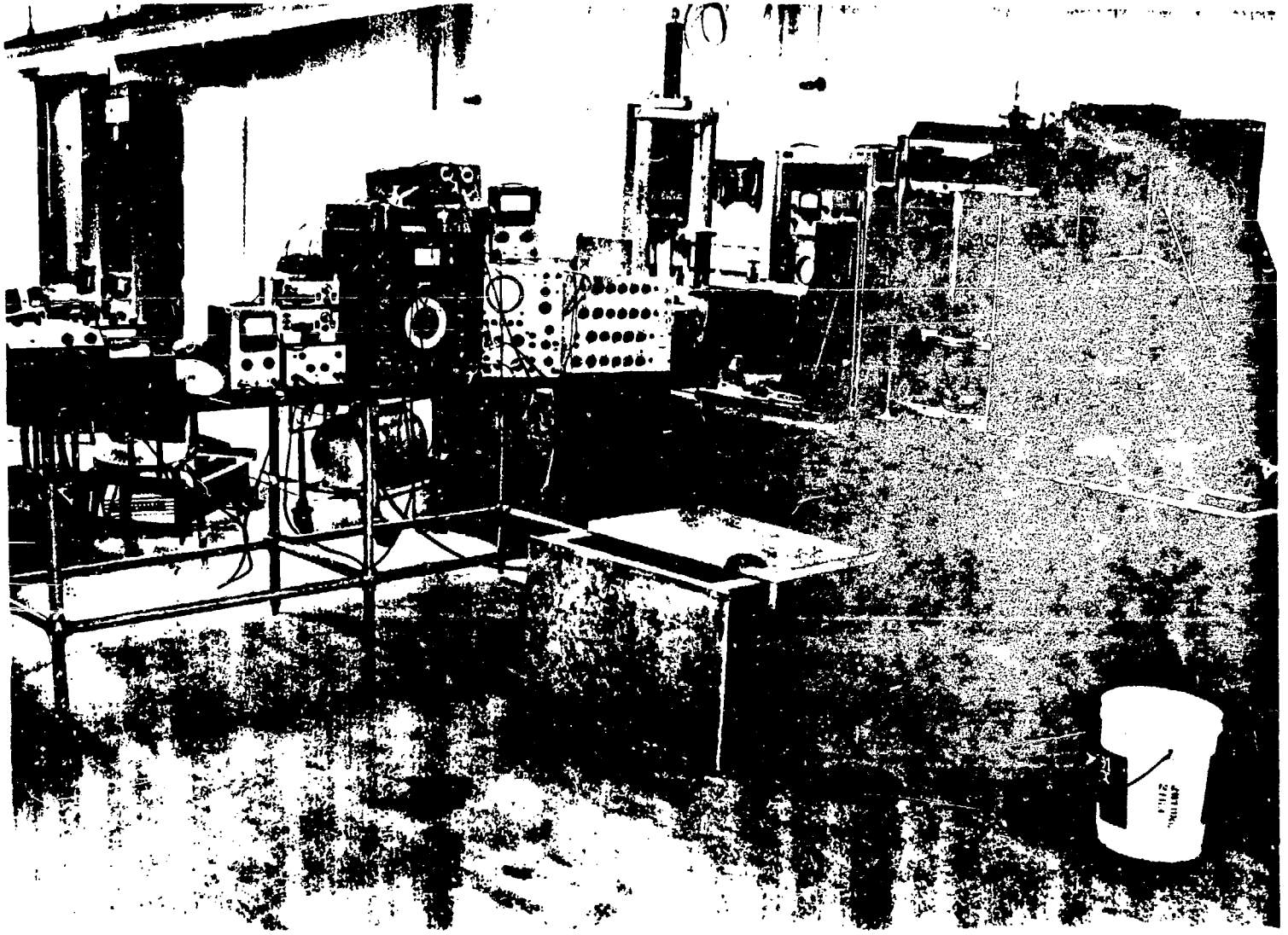

Figure 3 Resonant Frequency Experimental Setup

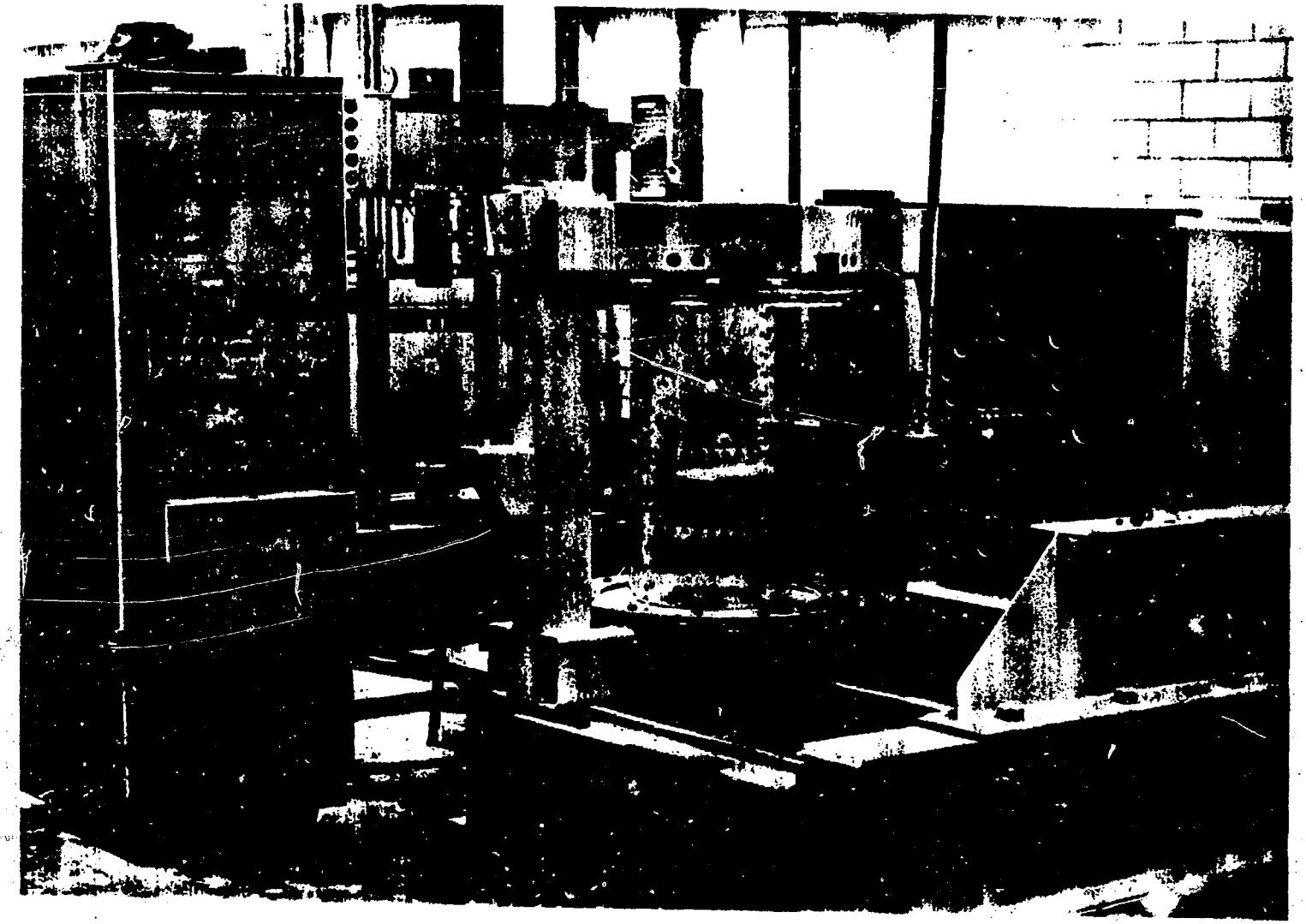

Figure 4 Overall View of Seismic Test Fixture and CGS Control Panel

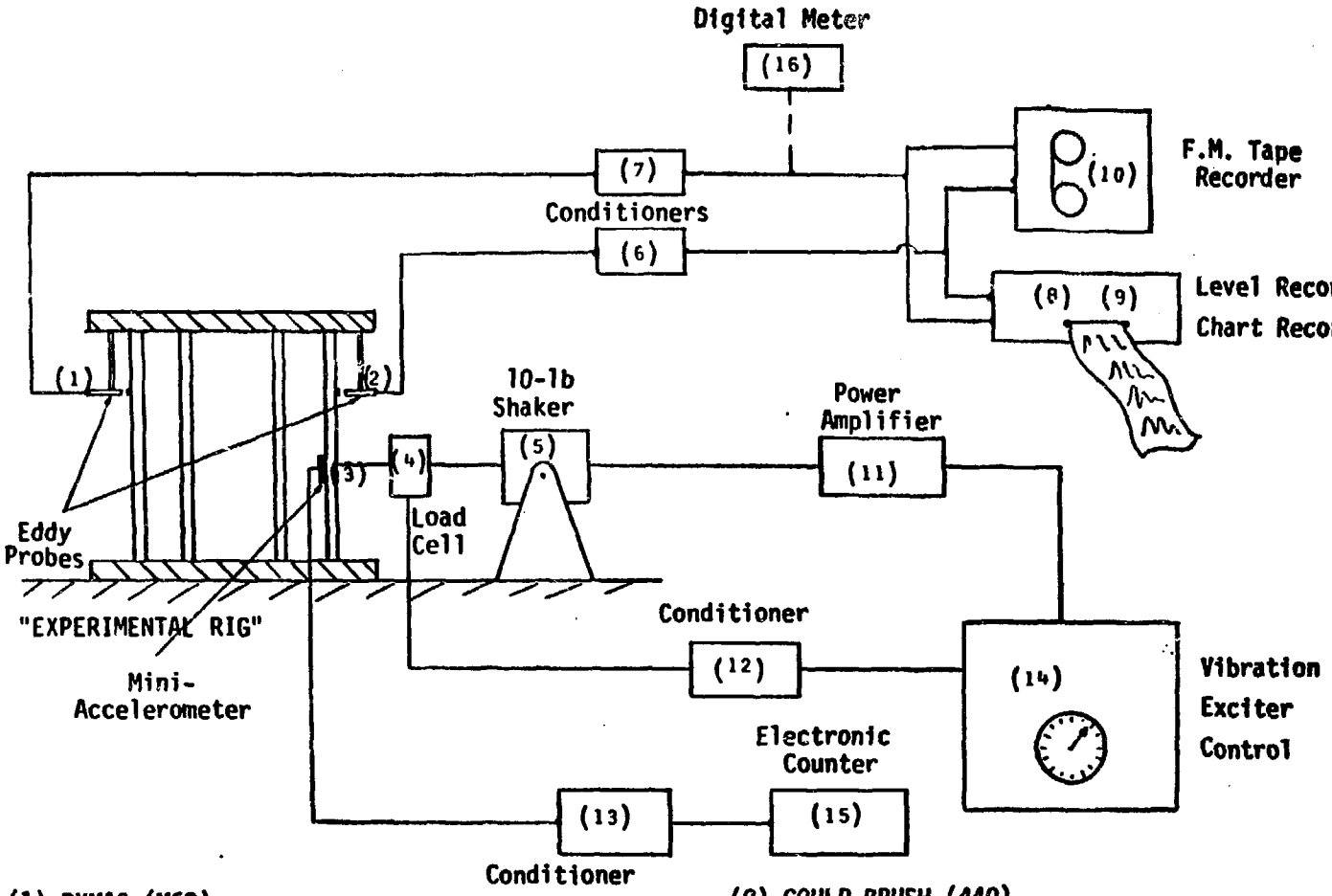

(1) DYMAC (M60)
(2) DYMAC (M60)
(3) B & K (8307)
(4) B & K (8200)
(5) B & K (4809)
(6) DYMAC (M600)
(7) DYMAC (M600)
(8) B & K (2305)
(9) GOULD-BRUSH (440)
(10) AMPEX (FR 1300-A)
(11) B & K (2706)
(12) B & K (2622)
(13) B & K (2622)
(14) B & K (1019
(15) HP (5512-A)
(16) KEITHLEY (168)

Figure 5 - Instrumentation for Natural Frequency and Mode Shape Determination

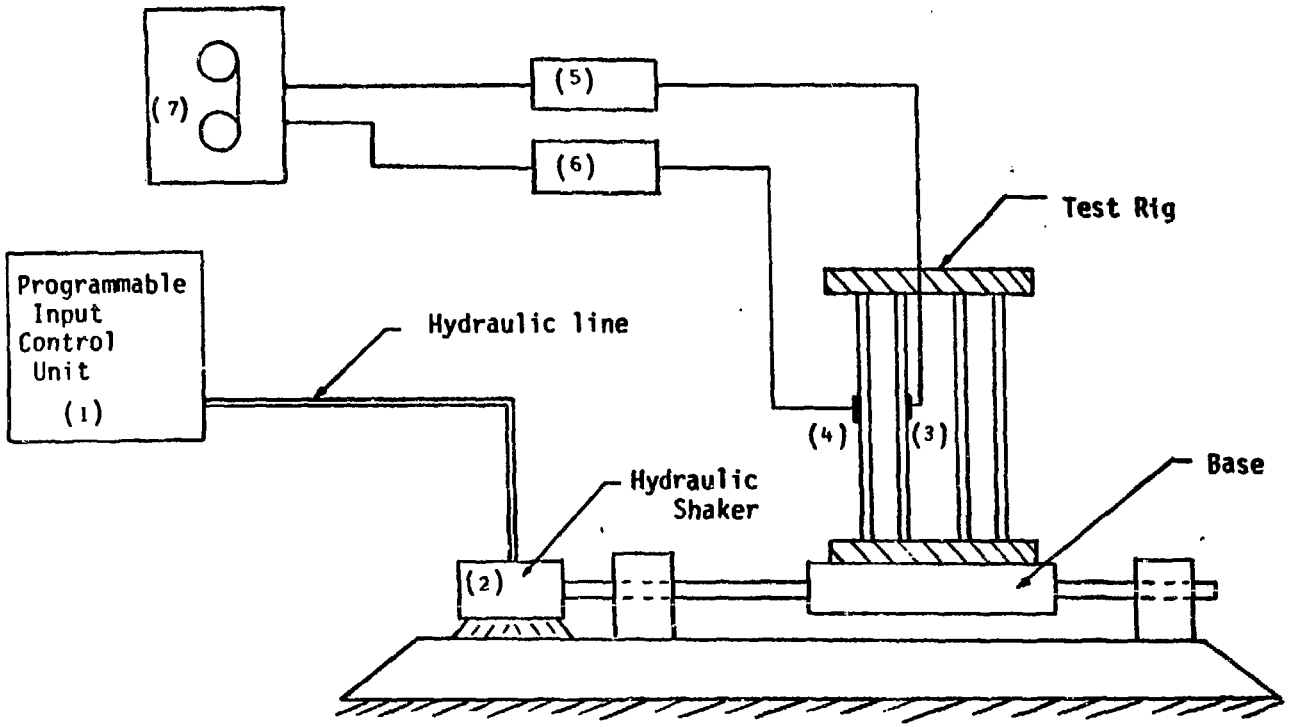

(1) Control Unit CGS/Lawrence (109-20)
(2) Actuator CGS/Lawrence (336)
(3) Mini-Accelerometer, B & K (8307)
(4) Mini-Accelerometer, B & K (8307)
(5) Conditioner, B & K (2622)
(6) Conditioner, B & K (2622)
(7) F.M. Recorder Ampex (FR 1300-A)

Figure 6 - Instrumentation for Seismic Experiment

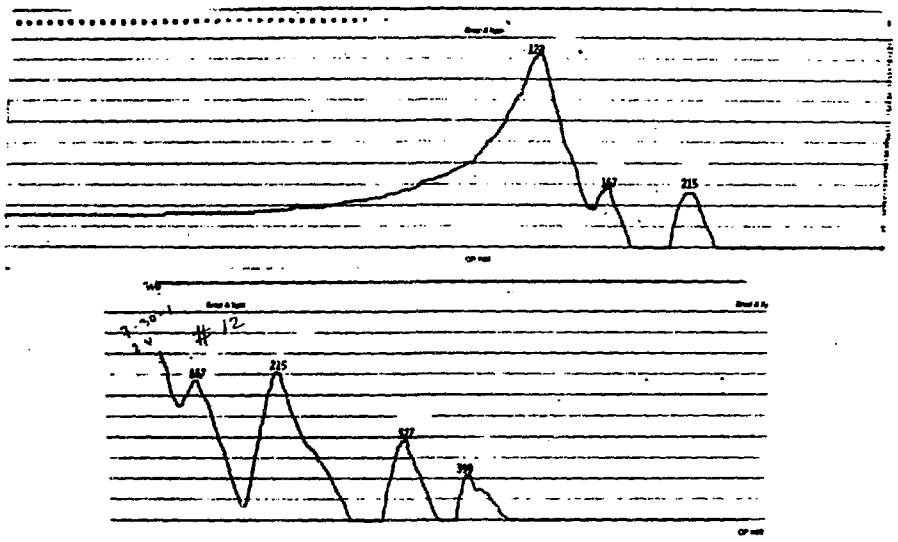

SPECTRUM

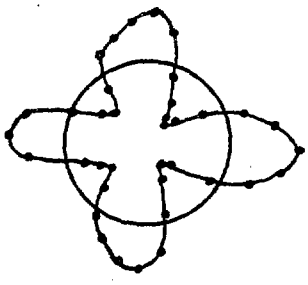

167 Hertz

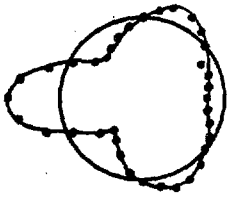

128 Hertz

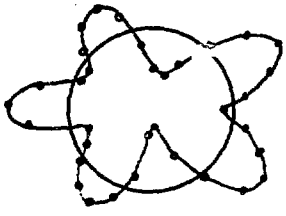

215 Hertz

MODE SHAPE

FIGURE 7 TYPICAL OUTPUTS

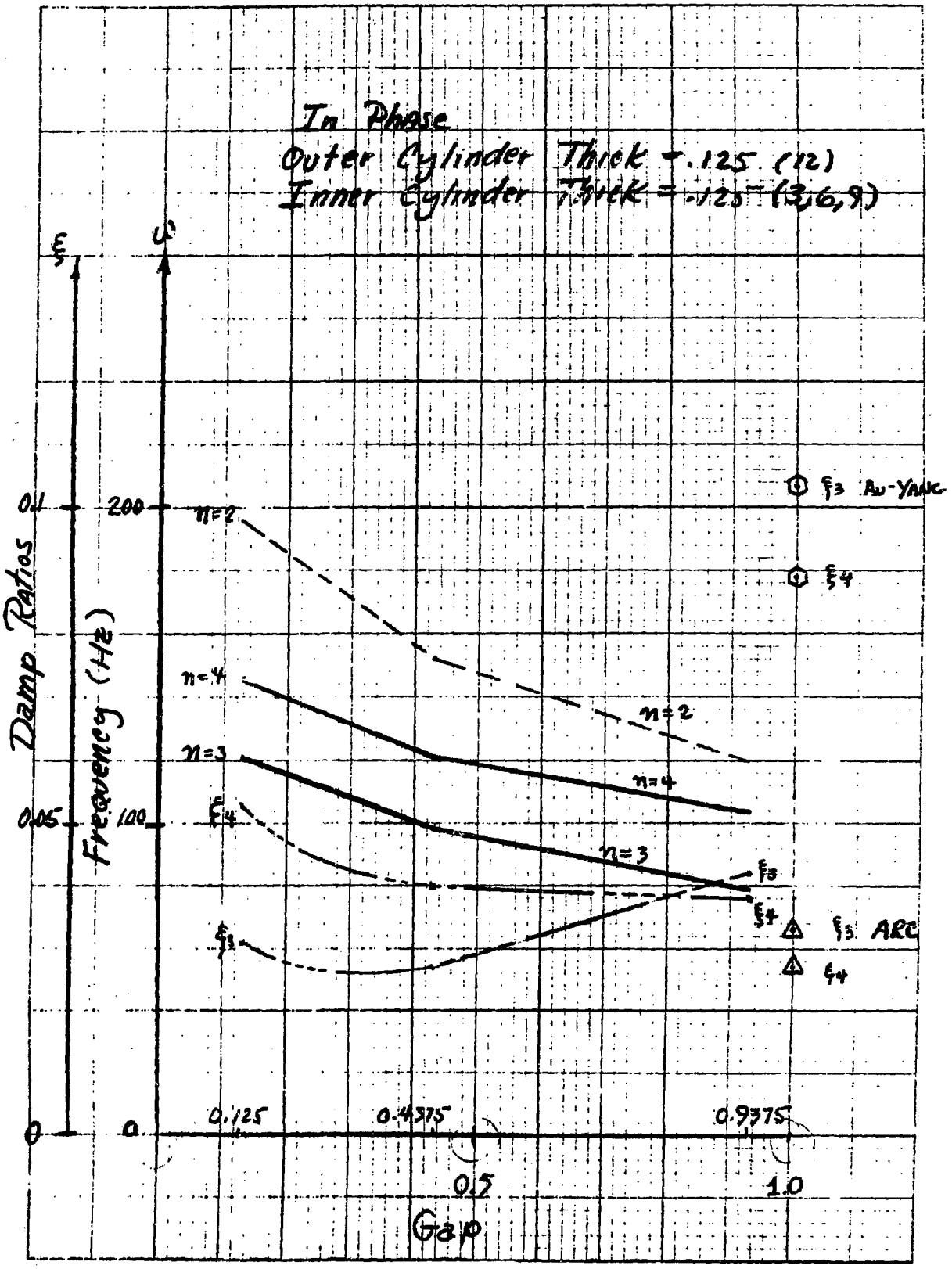
In Phase
Outer Cylinder Thick = .125 (12)
Inner Cylinder Thick = .125 (3,6,9)
ξ
ω
Damp Ratios
Frequency (Hz)
0.1
0.05
0
200
100
0
n=2
n=4
n=3
n=2
n=4
n=3
ξ4
ξ3
ξ3 Au-Yang
ξ4
ξ3
ξ4
ξ3 ARC
ξ4
0.125
0.4375
0.9375
0.5
1.0
Gap

Figure 8

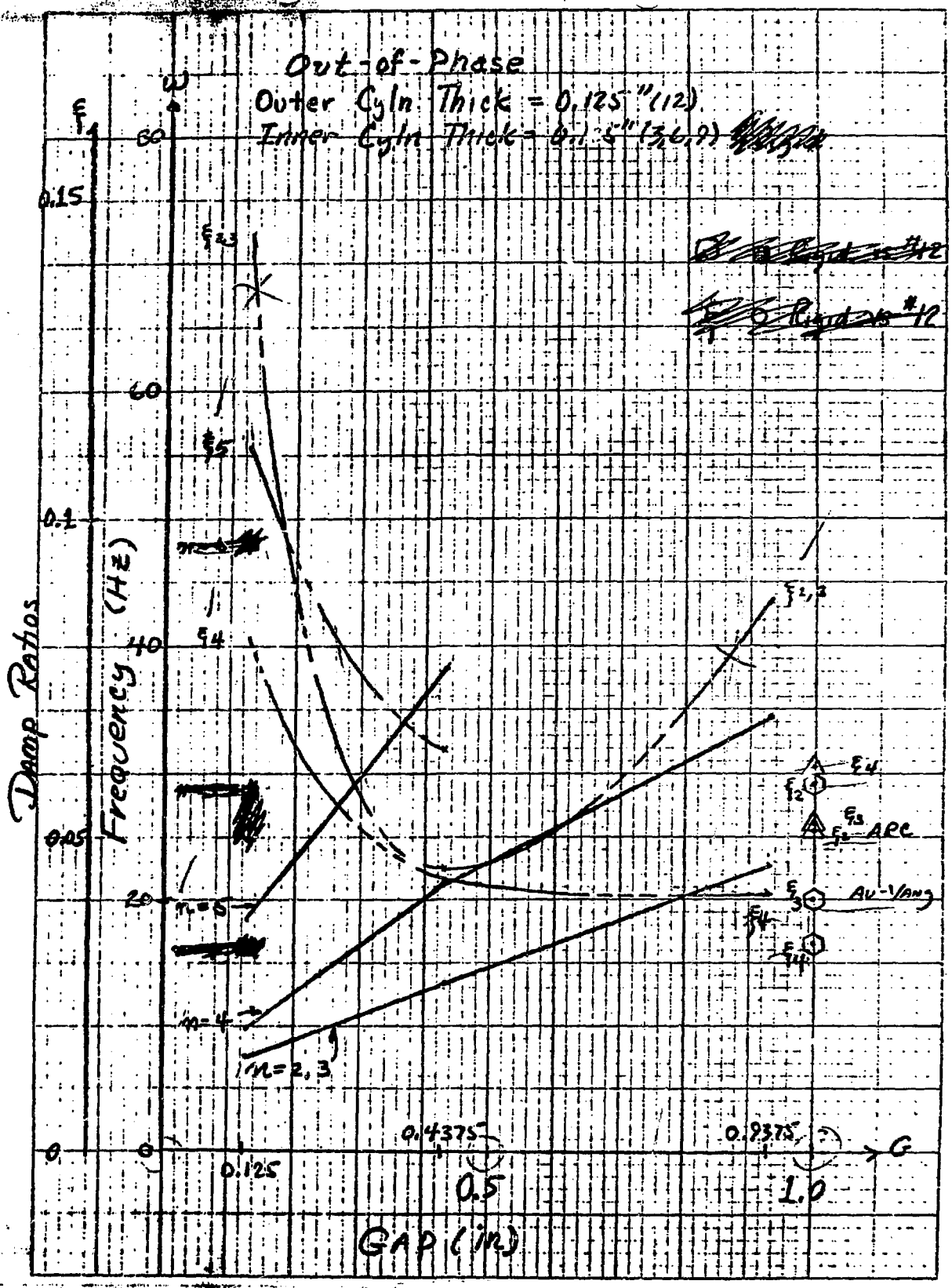
Out-of-Phase
Outer Cyln Thick = 0.125" (12)
Inner Cyln Thick = 0.15" (3,6,9)
Damp Ratios
Frequency (Hz)
ξ1
ω
60
40
20
0
0.15
0.1
0.05
0
ξ2,3
ξ5
ξ4
n=5
n=4
n=2,3
ξ1
ξ2
ξ3
ξ4
ξ5
ARC
AV-1/REV
0.125
0.4375
0.9375
0.5
1.0
G
GAP (in)

Figure 9

OUTER CYLINDER WITH INNER CYLINDER

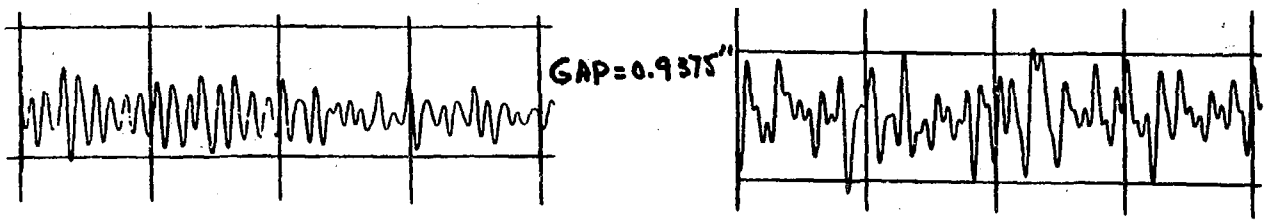

12 (O_3) 3 (I_{13})

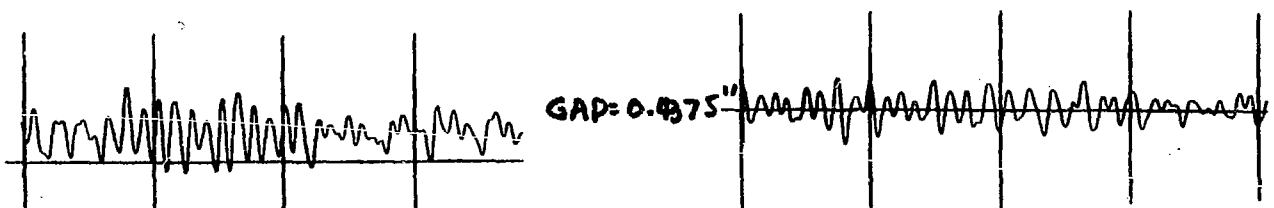

12 (O_3) 6 (I_{23})

12 (O_3) 9 (I_{33})

FIG. 10 RELATIVE ACCELERATION TIME RESPONSE

OUTER CYLINDER WITH INNER CYLINDER

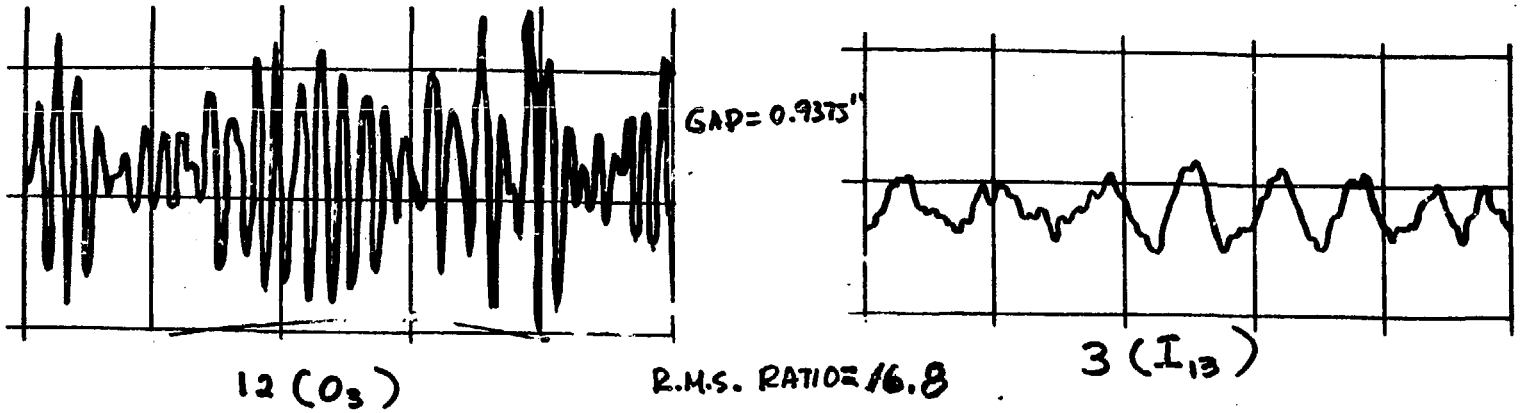

FIG. 11 RELATIVE DISPLACEMENT TIME RESPONSE

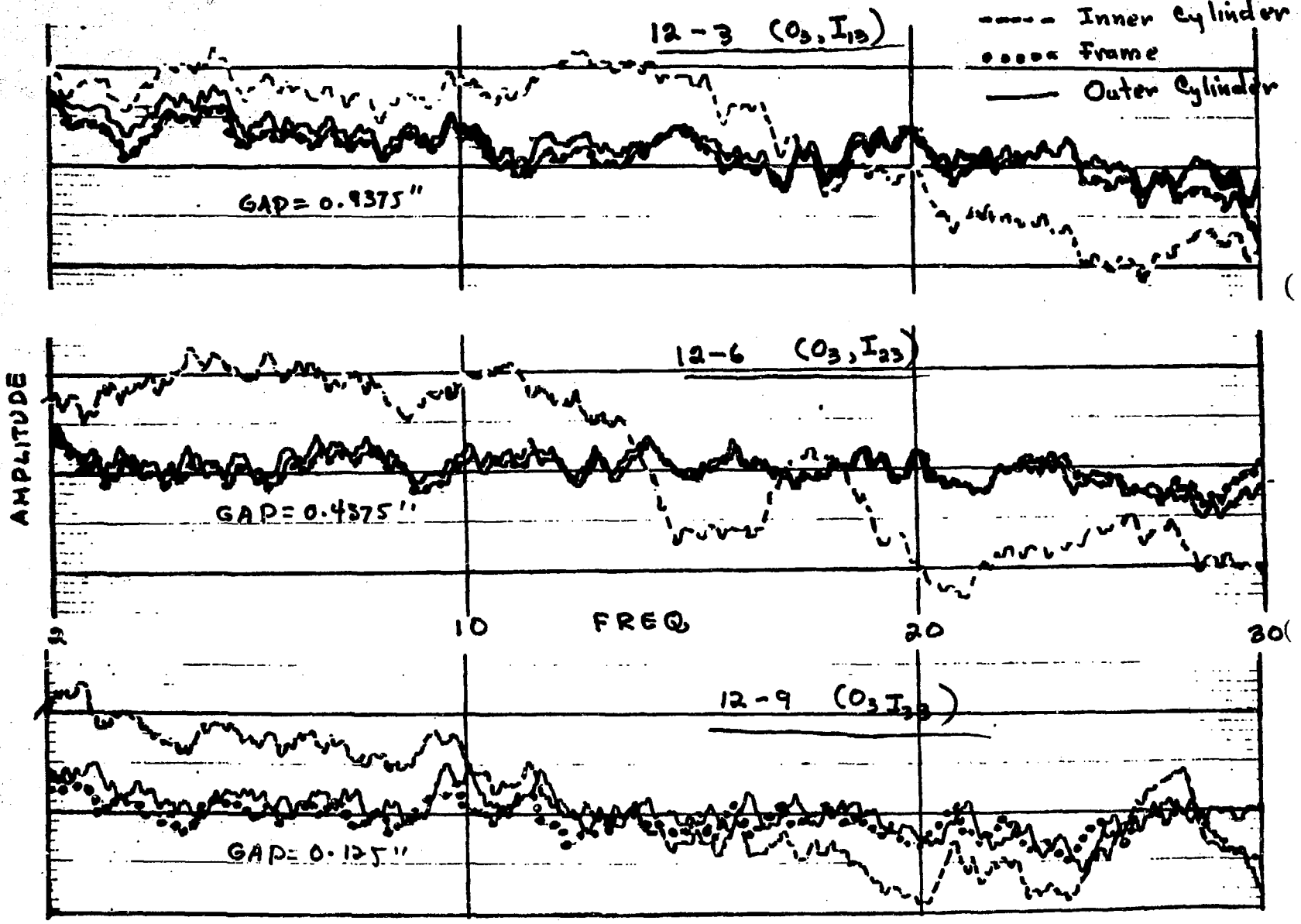

FIG. 12 FREQUENCY SPECTRUM